Published in IET Microwaves, Antennas & Propagation
Received on 25th May 2011
Revised on 12th April 2012
doi: 10.1049/iet-map.2011.0244



ISSN 1751-8725

Dual-band loop-loaded printed dipole array with a corporate balun/feed structure

A. Sondas M.H.B. Ucar Y.E. Erdemli

Electronics and Computer Education Department, Kocaeli University, Umuttepe Campus, 41380 Kocaeli, Turkey
E-mail: yunusee@kocaeli.edu.tr

Abstract: A novel loop-loaded printed dipole (LLPD) antenna array is introduced for a dual-band operation at 3.0/5.5 GHz bands. As the loop elements placed on the dipole aperture provide the dual-band operation, a new corporate balun/feed structure is employed to achieve balanced and matched excitation for the array. The simulation and measurement results for 1×1, 2×2 and 4×4 LLPD array designs are presented, demonstrating quite well agreement. In particular, the 4×4 design offers better than 17% impedance bandwidth and a realised gain of at least 15 dBi with tolerable side-lobe levels at the designated frequency bands.

1 Introduction

Multi-function antennas play a key role in today's communication systems where size, weight, power consumption and cost are the main limiting factors in designing integrated transmitter/receiver circuitry. Modern communication and radar applications particularly require the development of multiband or wideband arrays where those constraints become more critical. In this view, microstrip or printed antennas were previously employed in such applications because of their low-profile and rather manageable structures [1–8].

In this paper, we introduce a novel loop-loaded printed dipole (LLPD) array design for a dual-band operation at 3.0/5.5-GHz bands, which are designated for a specific radar application. Although the loop elements placed on the dipole aperture provide the dual-band operation, a new corporate balun/feed structure is employed for the array excitation. Parasitic or loading elements have been considered in recent dipole studies to obtain multiband or broadband operation [9–13]. In particular, a dual-band printed dipole antenna with a multi-arm parasitic element is introduced in [10] for WiMAX applications covering the bands 2.5–3.8 and 5.15–5.85 GHz where an average directivity of 2 dBi is realised. In [12], an antipodal printed dipole loaded with circular split-ring resonator (SRR) elements has been introduced for a dual-frequency operation. In that study, eight SRR elements consisting of two concentric split-rings each are placed along the length of the dipole to achieve a dual-band operation at 1.2 and 2 GHz bands. The SRR elements there play a key role in occurrence of the higher-band where a rather low gain (~1 dBi) with a moderate efficiency (~70%) is obtained. In another study reported in [13], a double-sided crossed dipole with four parasitic square split-ring elements is proposed for a broadband circularly polarised array application. The 2×2 crossed-dipole array design, in particular, provides 3-dB axial-ratio over 1.95–3.45 GHz band where two split VSWR < 2 bandwidths (~41 and 5.9%, ~2.4 and at 3.2 GHz, respectively) are realised with the directivity levels of 5–15 dBi.

In this research, we propose a novel printed dipole antenna loaded with two rectangular loop elements (without splits) asymmetrically placed along the dipole length to achieve the dual-band array operation around the centre frequencies of 3 and 5.5 GHz. As compared to its counterparts mentioned above, the proposed LLPD configuration is rather simple in structure, yet offers more flexibility in designing for different operational frequencies while maintaining the desired antenna operation. It is also important to point out that in achieving the optimum antenna performance, a wideband balanced and matched excitation is particularly essential, and this can be achieved by means of an appropriate balun/feed structure compatible with the dipole configuration [14–16]. We have preferred to employ a balun/feed design similar to that of [15] because of its low profile and its easy integration with the array antenna. In addition, a new corporate feed network integrated with the wideband balun/feed structure is employed for the LLPD array excitation, which is also a key contribution of this research. The obtained results show that the type of balun along with the feed network used here meets the requirements quite well for the array application at hand. In particular, the 4×4 LLPD array offers a minimum of 17% impedance bandwidth with a realised gain of at least 15 dBi at the designated frequency bands. We remark that the proposed low-profile LLPD design along with the corporate balun/feed network can easily be adapted for different operational frequencies to be considered in various communications applications.

In the paper, the simulation (input reflection coefficient, i.e. S_{11}, gain, pattern) and measurement (S_{11}, pattern) results for

© The Institution of Engineering and Technology 2012

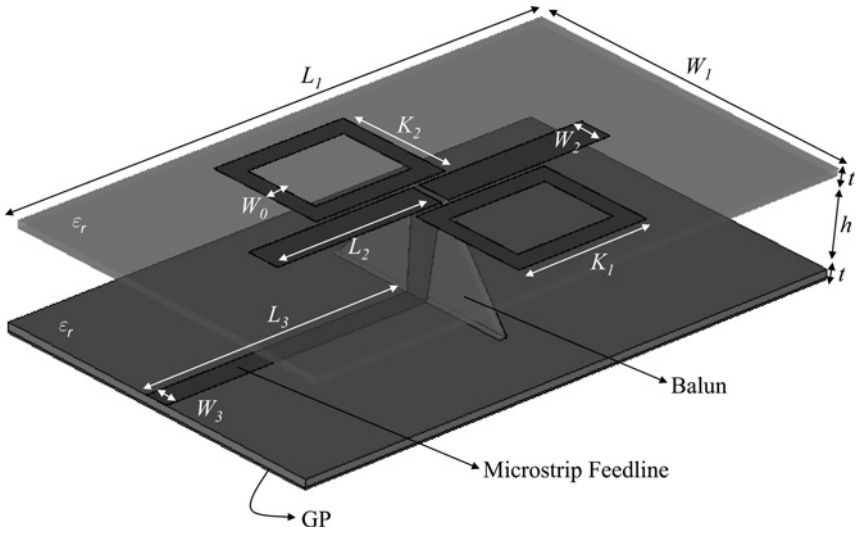


Fig. 1 *LLPD antenna configuration: $W_1 = 36$, $L_1 = 66$, $W_2 = 3.5$, $L_2 = 20.6$, $W_3 = 2.4$, $L_3 = 32.6$, $K_1 = 16.25$, $K_2 = 12.4$, $W_0 = 2.1$, $h = 9.2$, $t = 0.79$ (all in mm), $\varepsilon_r = 2.2$*

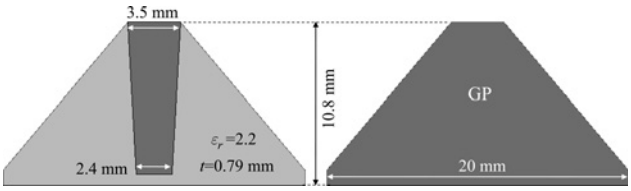


Fig. 2 *Balun configuration: the front side (left) and the back side (right)*

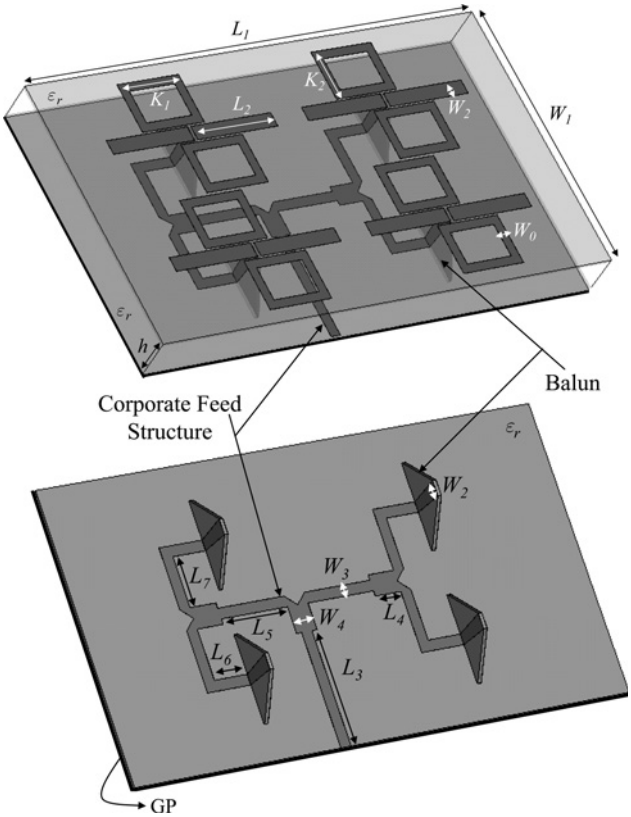


Fig. 3 *2×2 LLPD array configuration: $L_1 = 116$, $W_1 = 66$, $K_1 = 15.75$, $K_2 = 12.4$, $W_0 = 2.1$, $L_2 = 20.6$, $W_2 = 3.5$, $h = 9.2$, $L_3 = 25.8$, $L_4 = 6$, $L_5 = 15.4$, $L_6 = 7.6$, $L_7 = 11.4$, $W_3 = 2.4$, $W_4 = 4.8$ (all in mm), $\varepsilon_r = 2.2$*

1×1, 2×2 and 4×4 LLPD array designs are presented. We note that the full-wave analysis of the proposed designs has been carried out using CST Microwave Studio, which is a well-known electromagnetic (EM) simulator utilising the finite-integration technique in time domain. Also note that this paper is the comprehensive version of the study reported in [17], that is, here we additionally present the 4×4 array design along with the corresponding measurements for all the designs considered.

2 LLPD array designs

The single-element (1×1) LLPD configuration is depicted in Fig. 1 along with the corresponding physical parameters. As seen, the antenna aperture consists of a printed dipole and a pair of loop elements asymmetrically located (at a distance

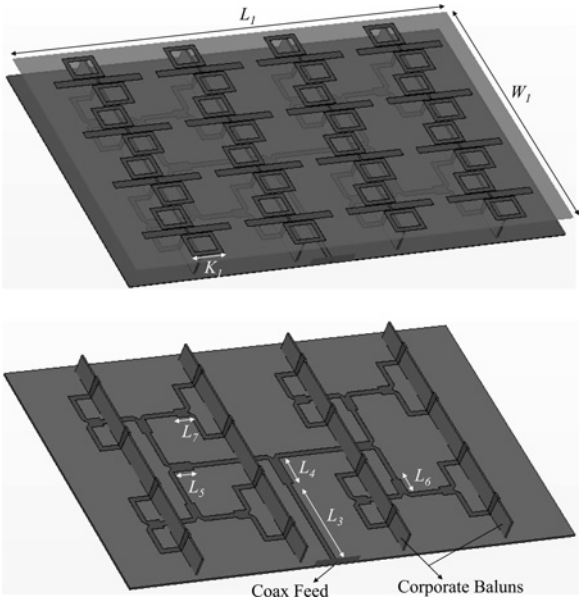


Fig. 4 *4×4 LLPD array configuration: $L_1 = 216$, $W_1 = 126$, $K_1 = 15.25$, $L_3 = 46.8$, $L_4 = 15$, $L_5 = 10$, $L_6 = 8$, $L_7 = 6$ (all in mm); all other parameters are same as those of the 2×2 LLPD array*

© The Institution of Engineering and Technology 2012

doi: 10.1049/iet-map.2011.0244

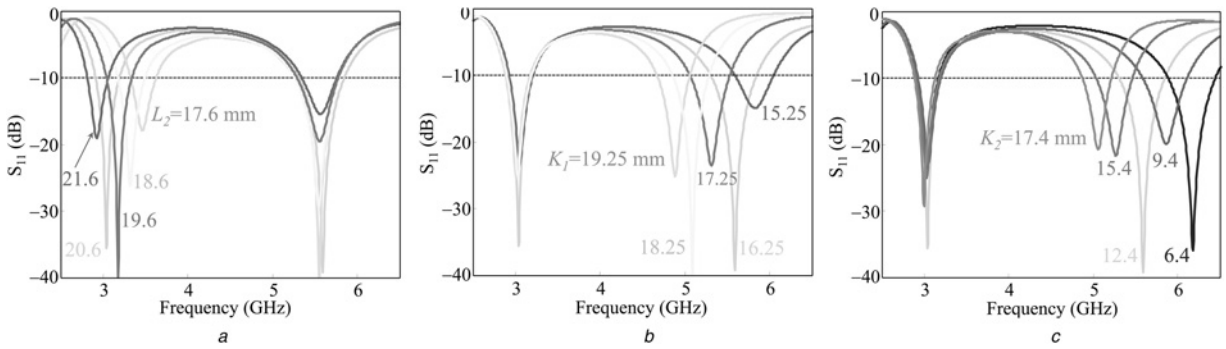


Fig. 5 *Effects of*

a Dipole length ($2L_2$)
b Loop dimensions K_1 and
c K_2 on the S_{11} performance

of 0.5 mm) at each side of the dipole feed-gap, which is 0.89 mm. All these elements are supported by a thin substrate with $t = 0.79$ mm and $\varepsilon_r = 2.2$ (Arlon DiClad 880) and placed over an air layer of height $h = 9.2$ mm. We note that the critical parameters to achieve the desired dual band performance at the designated frequency bands (3/5.5 GHz) are the cavity height, the dipole size, the loop dimensions and their location with respect to the dipole element. As the dipole length mainly determines the lower-band, the loop elements play a crucial role in occurrence of the higher-band. The loop elements provide not only inherent inductive but also capacitive loading, which is because of proximity of each loop to the dipole. Hence, these parasitic ring elements help in impedance matching as well.

As shown in Fig. 1, the LLPD antenna is excited by a microstrip balun-feed structure placed vertically just

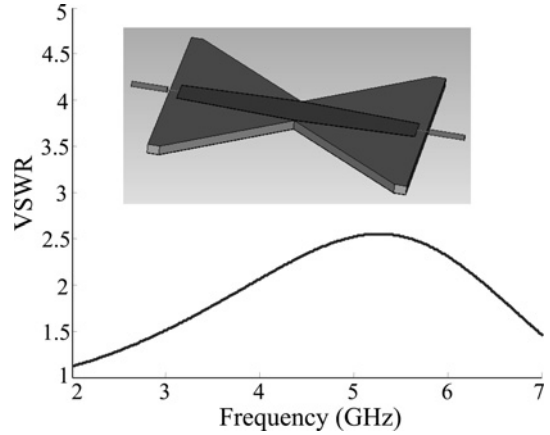


Fig. 6 *Simulated VSWR characteristics of the back-to-back balun structure*

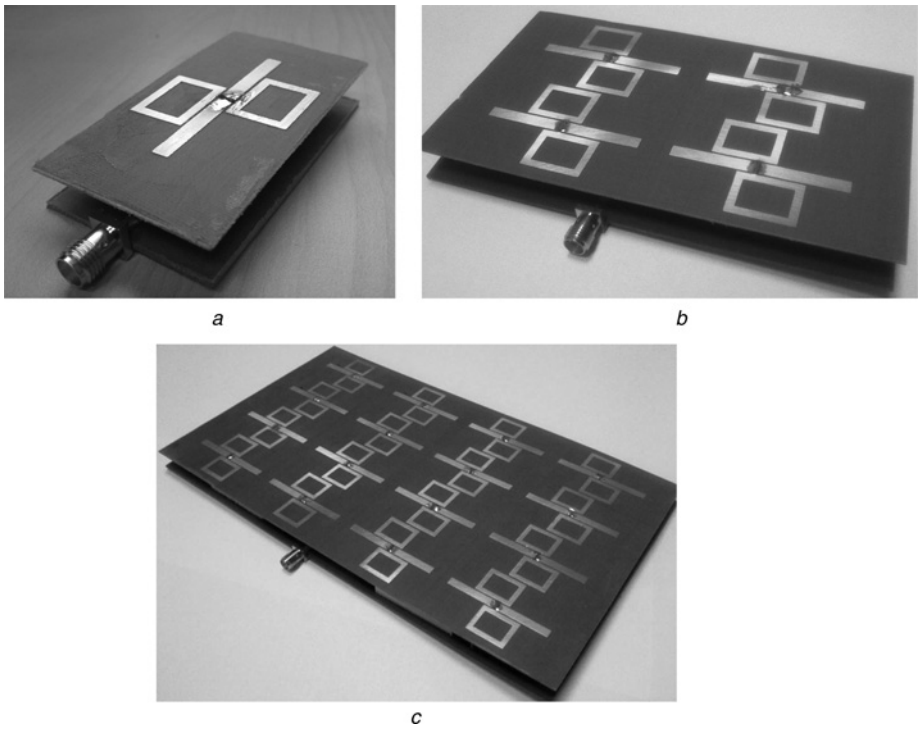


Fig. 7 *Fabricated LLPD arrays*

a 1 × 1
b 2 × 2
c 4 × 4

© The Institution of Engineering and Technology 2012

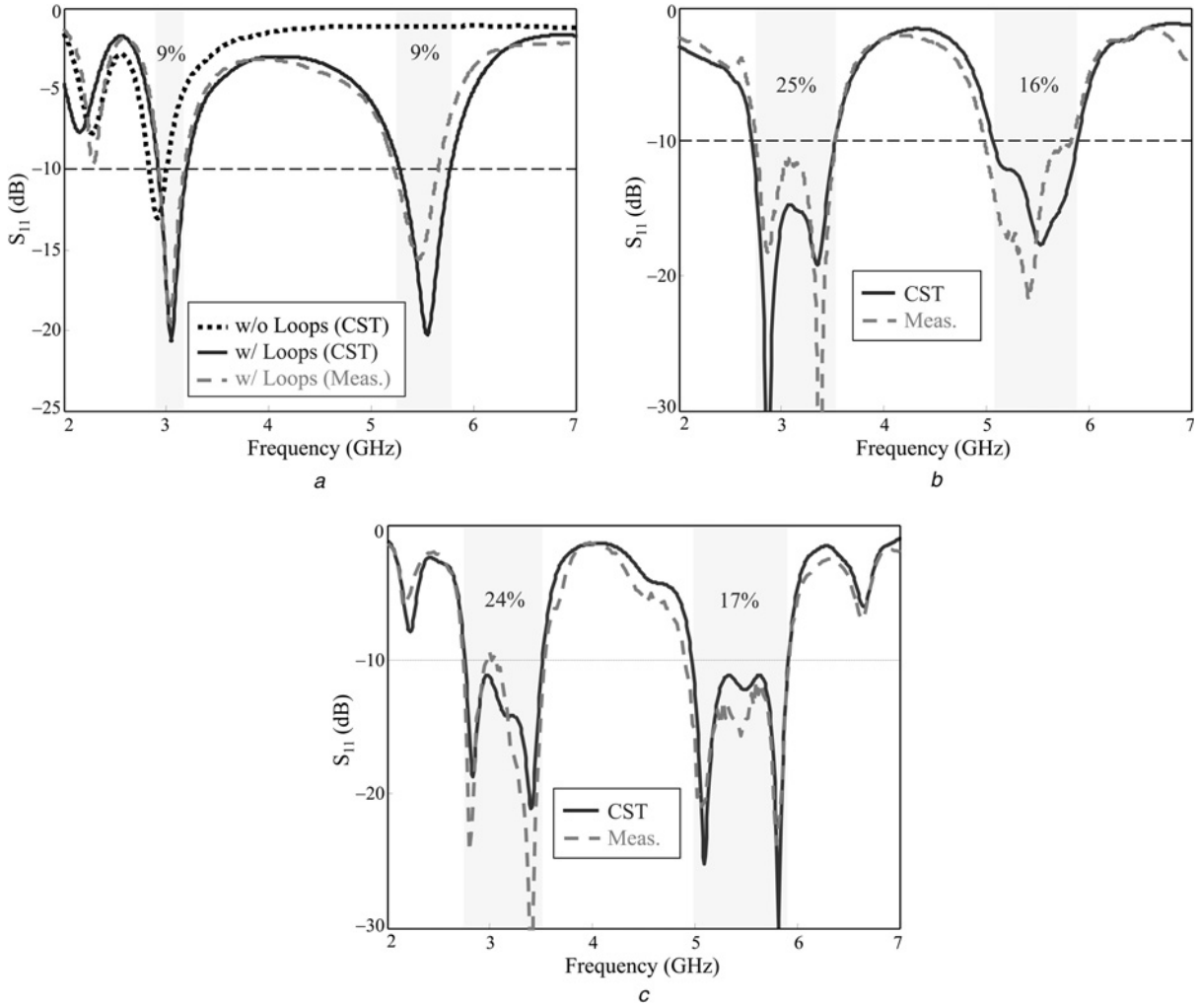


Fig. 8 *S_{11} characteristics of LLPD designs: measurements against CST simulations*

a 1×1
b 2×2
c 4×4

underneath the dipole-gap. We remark that the dipoles cannot perform in the way as predicted when they are excited directly by a coaxial feed [18], which is because of inherit unbalanced current excitation by the coax. To overcome this undesired phenomenon, a balun (balanced-to-unbalanced) structure is required in the coax-fed dipole applications in order to match the unbalanced coaxial transmission line to the balanced two-wire line, that is, the dipole in our case. Hence, a new balun structure having compatible conjunction with the dipole has been designed. The balun structure has a tapered microstripline and is supported by a thin substrate ($t = 0.79$ mm, $\varepsilon_r = 2.2$) placed on a triangular-shaped ground plane (GP) as depicted in detail in Fig. 2. The triangular shape is chosen to accommodate the balun structure underneath the dipole gap appropriately [15]. As also seen from Fig. 2, the width of the balun's microstripline widens linearly from the lower-end to the aperture level, where the corresponding characteristic impedance of the line varies from 50 to 40 Ω, respectively. In addition, the balun's microstripline at the lower-end is connected to a 50-Ω microstrip feedline extending along the dipole length to the coax-end. This feeding line is also supported by a similar substrate backed by the GP.

In light of the single-element LLPD design described above, 2×2 and 4×4 LLPD arrays have been designed as shown in Figs. 3 and 4, respectively. Although extending the 1×1 array to its 2×2 and then 4×4 counterparts, the dipole and loop dimensions have been slightly changed during optimisation process to achieve the desired dual-band performance. Note that there has been no change in the balun parameters, which are kept the same as of the single-element LLPD. Also note that in the 4×4 array, each group of four balun elements in the *H*-plane share the same substrate for a rather sturdy integration of the baluns within the cavity. It is important to note that a new corporate feed structure has been designed to excite the array elements appropriately. As can be seen from Figs. 3 and 4, the feed structure has only one coax input which is distributed to the balun structures via microstrip feeding lines, each of which has the same length to achieve in-phase excitation for the array elements. The feeding lines, on the other hand, have different widths (realising ~30 Ω characteristic impedance) at the junctions for a better matching to 50-Ω system. We remark that the proposed corporate-feed configuration is simple in structure and can easily be adaptable to arrays with $2^n \times 2^n$ elements ($n \geq 1$).

© The Institution of Engineering and Technology 2012

doi: 10.1049/iet-map.2011.0244

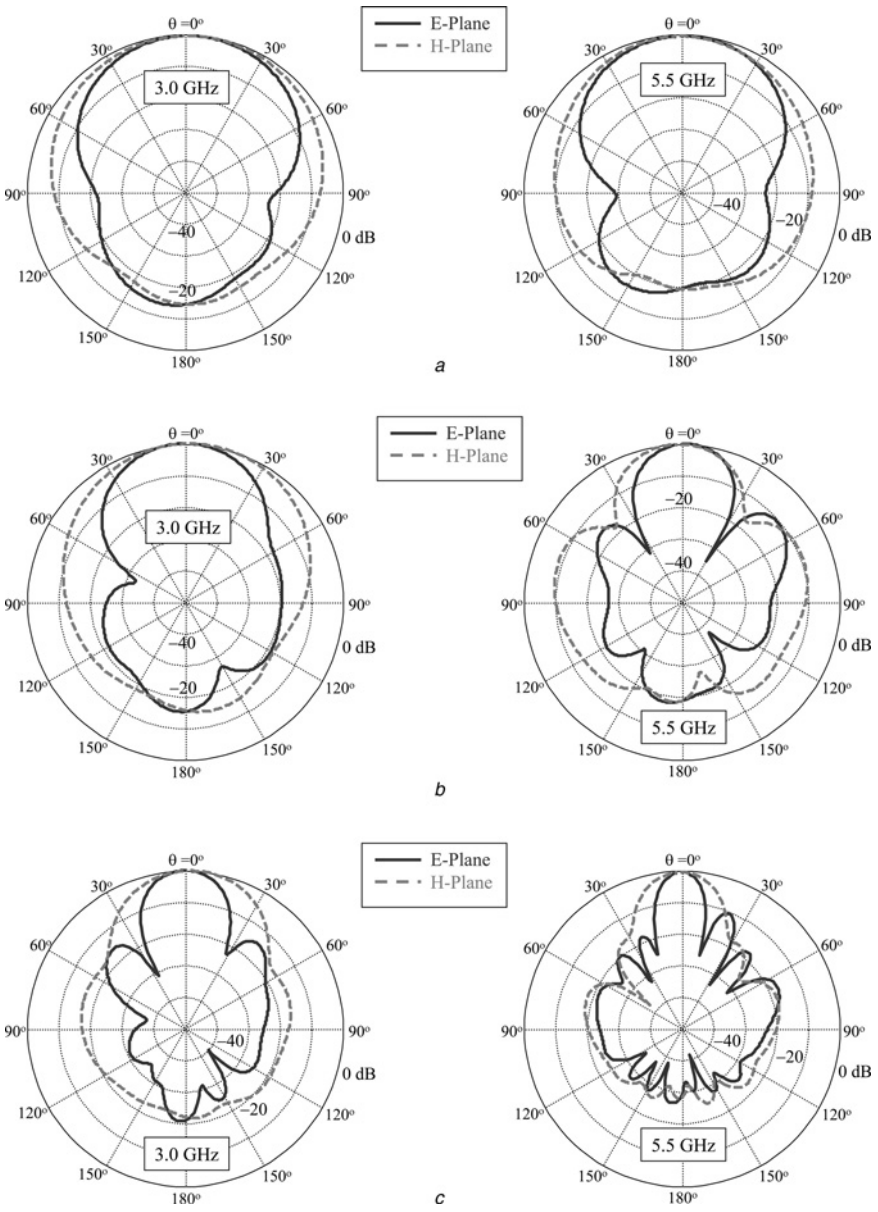


Fig. 9 *Computed E- and H-plane radiation patterns of LLPD designs at 3 and 5.5 GHz*

a 1 × 1
b 2 × 2
c 4 × 4

3 Results and discussions

In this section, we will present the simulated and measured results for the proposed LLPD arrays. Prior to that we first present several parametric studies carried out during the design process which led to the optimum LLPD design. As representative examples, here we demonstrate the effects of the dipole length ($2L_2$) and the loop dimensions (K_1 and K_2) on the S_{11} performance. As can be seen from Fig. 5, the dipole length mainly determines the lower-band, while the loop dimensions play a major role in occurrence of the higher-band. Of importance is that when the dipole length is fixed, by varying the loop size one can shift the higher-band upwards or downwards with an insignificant effect on the lower-band. Similarly, by varying the dipole length with the loop size fixed, one can shift the lower-band accordingly. These studies prove the flexibility of the proposed design.

In another study, by varying the distance between the rings along the dipole length (i.e. the loops become closer to the dipole ends or the dipole centre), it has been observed that both frequency bands slightly shift (at most 5%) downwards or upwards, respectively. Also, as the gap between each loop and the dipole is increased, the S_{11} levels increase, that is, the impedance matching worsens. In light of those parametric studies, the optimum design parameters were finally obtained as given in Fig. 1.

Before presenting the performance of the optimum LLPD designs, we first consider the simulated balun performance as displayed in Fig. 6. As seen, the back-to-back balun structure provides VSWR < 2.5 over the band of interest (2–7 GHz). Despite those slightly high VSWR levels (as compared with the standard criteria of VSWR < 2), the proposed balun design is rather low-profile and meets the requirement of matched and balanced excitation for the LLPD arrays quite well. This balun design has been realised underneath the 1 × 1, 2 × 2 and 4 × 4 LLPD arrays as displayed in Figs. 1, 3 and 4 along with their fabricated prototypes as depicted in Fig. 7.

© The Institution of Engineering and Technology 2012

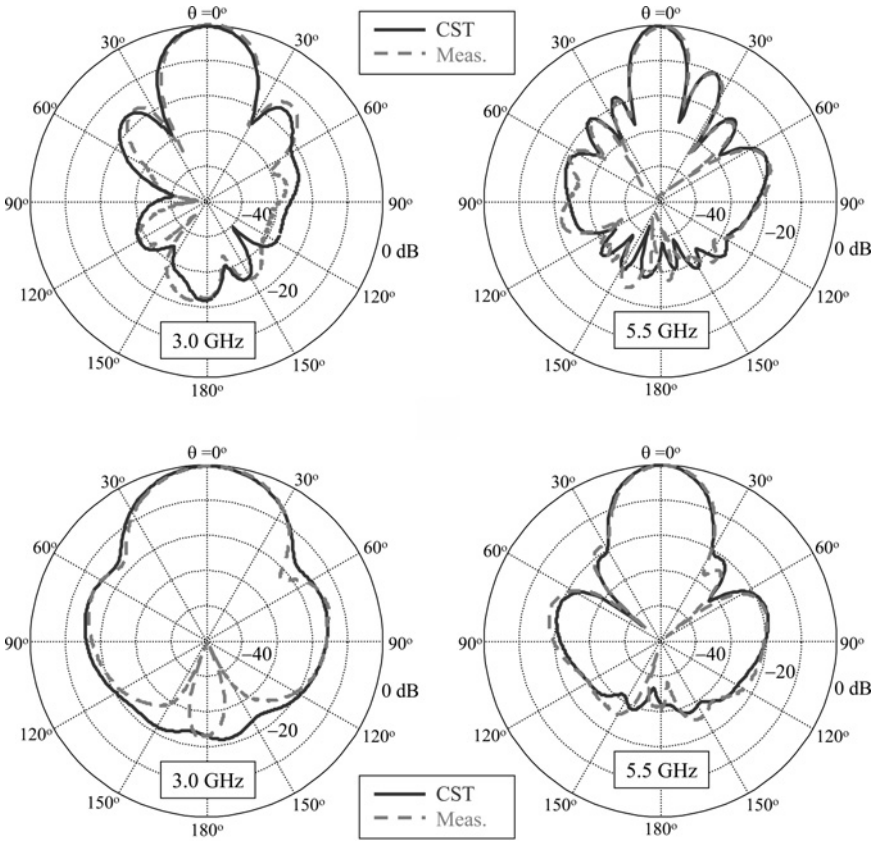


Fig. 10 *Normalised E-plane (top) and H-plane (bottom) patterns for the 4 × 4 LLPD array at 3 GHz (left) and 5.5 GHz (right): measurements against CST simulations*

The input reflection coefficients of the simulated and fabricated 1 × 1, 2 × 2, 4 × 4 LLPD arrays are displayed in Fig. 8. As shown in Fig. 8*a*, the single-element LLPD design offers a dual-band operation at the designated frequency bands around 3 and 5.5 GHz with a 9% impedance bandwidth each. In the same figure is also displayed the simulated design without loop elements for comparison purposes. As seen, the ring elements allow for the occurrence of the higher-band, while the dipole by itself is responsible for the lower-band. The projected dual-band performance is also observed for the 2 × 2 and 4 × 4 LLPD designs with improved S_{11} bandwidth performance, which is mainly owing to the proposed corporate feed structure as well as coupling between the array elements. In particular, each of those designs offers at least 24 and 16% S_{11} bandwidths for 3 and 5.5 GHz bands, respectively, as shown in Figs. 8*b* and *c*. Note that the bandwidth performance stated here is based on the criterion $|S_{11}| < -10$ dB (equivalently VSWR < 2) where a 50-Ω system is considered. We remark that the agreement between the measured and simulated S_{11} characteristics is quite good except insignificant differences in S_{11} levels and slight frequency shifts, which are probably because of material and fabrication tolerances. Of importance, here is that the realised LLPD arrays result in the expected dual-band operation at the designated frequency bands. Also note that the input reflection coefficient measurements were carried out using Rohde and Schwarz ZVB8 Vector Network Analyser.

In addition, we present the computed radiation characteristics of the proposed LLPD designs in Fig. 9 where the *E*-plane and *H*-plane broadside radiation patterns are displayed for the LLPD arrays at 3 and 5.5 GHz. In particular, the 1 × 1 design has almost dipole-like *E*-plane patterns with a directivity of about 7.4 dBi at the respective frequencies. As expected, the side lobes appear in the patterns for the 2 × 2 and 4 × 4 arrays, particularly, the maximum side-lobe level (SLL) occurs as −8 dB in the *H*-plane for the former array, and −10 dB in the *E*-plane for the latter array, both at 5.5 GHz. In addition, the computed cross-polarisation levels at broadside are −20, −15 and −12 dB for the 1 × 1, 2 × 2 and 4 × 4 arrays, respectively, at 3 and 5.5 GHz. Moreover, we carried out radiation pattern measurements for the 4 × 4 LLPD array in an anechoic chamber using ETS-Lindgren 3117 DRG horn antenna (1–18 GHz). The corresponding measured patterns at 3 and 5.5 GHz along with the simulated data are displayed in Fig. 10 where a reasonably well agreement is observed.

Furthermore, the computed realised gain (IEEE gain × mismatch losses) characteristics of the arrays are displayed in Fig. 11. As shown, the 2 × 2 array offers around 10 and 14 dBi gain, whereas the 4 × 4 array results in ∼15 and 19 dBi gain at 3.0 and 5.5 GHz bands, respectively. As also observed from Fig. 11, each gain profile has a gain-dip between the respective bands, emphasising the dual-band operation. In addition, the measured gains for the 4 × 4 array are ∼14.3 and 19 dBi at 3.0 and 5.5 GHz, respectively, which are almost the same as the respective simulated gains. Also note that the computed radiation efficiencies for all of the designs considered is better than 90%.

Subsequently, the array's radiation performance (SLL and gain characteristics) against mutual coupling is discussed in a

© The Institution of Engineering and Technology 2012

doi: 10.1049/iet-map.2011.0244

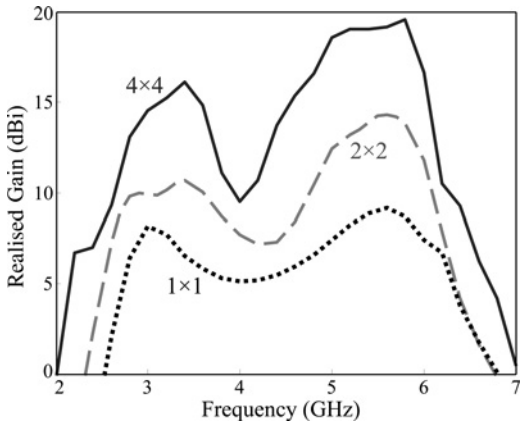


Fig. 11 *Computed realised gain characteristics of the LLPD arrays*

qualitative manner. The coupling is mainly controlled by the separation between the array elements in both *E*- and *H*-plane. The parametric studies reveal that as the *H*-plane separation (i.e. the loop dimension K_2; Fig. 3) is increased, the corresponding SLL also tends to increase, particularly, in the upper band (5.5 GHz). In addition, as can be seen from Fig. 11, the gain levels in the upper-band are almost 3 dB higher than those in the lower-band for the array designs unlike the single element (1 × 1) design where the gain levels are comparable over the bands of interest. This is probably because of the fact that not only does the array become electrically larger, but also the mutual coupling is alleviated (possibly owing to the loop elements) at the higher frequencies, thus enhancing the gain performance. Also note that the gain is increased ~6 dB in both operational bands when the array is extended from 2 × 2 to 4 × 4, as expected, with noting that the respective array parameters are slightly different. To demonstrate the effect of loop elements on the radiation characteristics, we have also simulated the 4 × 4 array (Fig. 4) in absence of loop elements for comparison purposes. It has been observed that the SLL in the *H*-plane patterns is improved by almost 3 dB (on the average) in the upper band by inclusion of the loop elements as compared to the no-loop case. However, there is no significant improvement or degradation observed in the lower band (3 GHz) because of the loop elements. Moreover, the presence of loop elements enhances the directivity by almost 1 dB in the upper-band. Those analyses demonstrate that the loop elements not only improve the impedance matching in both bands (Fig. 8), but also help in alleviating the mutual coupling between array elements, thus improving the SLL as well as the gain, particularly in the higher frequency-band.

4 Conclusion

In this paper, we have introduced a novel LLPD antenna for dual-band array applications. The proposed design has two key features: as the loop elements placed on the aperture provides dual-band operation at the designated frequencies, the corporate balun/feed structure allows for matched and balanced excitation for the array. The 1 × 1, 2 × 2 and 4 × 4 LLPD arrays were designed via the CST simulator, and the corresponding prototypes were fabricated. It has been demonstrated that the simulations agree quite well with the measurements. In particular, the 4 × 4 design offers 24 and 17% S_{11} bandwidths at 3 and 5.5 GHz bands, respectively, and demonstrates a dual-band gain profile with the predicted gain values better than 15 dBi over the bands of interest. In addition, the corresponding side-lobe levels, cross-polarisation levels at broadside, and front-to-back ratios are better than −10, −12 and 20 dB, respectively, at those particular frequencies. We remark that the proposed low-profile array antenna with the corporate balun/feed is rather simple in structure and can easily be adapted for different operational frequencies to be considered in diverse communications applications.

5 Acknowledgments

This work has been supported by the Scientific and Technological Research Council of Turkey (TUBITAK Project No. 107E198) and partly funded by the Scientific Research Projects Unit of Kocaeli University (Project No. 2010/35). The authors thank Dr Fatih Ustuner, Mr Mustafa Dogan and Mr Sefa Ogan from TUBITAK/UEKAE laboratory for their invaluable assistance during fabrication and measurements. We also thank the anonymous reviewers for their invaluable comments.

6 References

1 Pokuls, R., Uher, J., Pozar, D.M.: 'Dual-frequency and dual-polarization microstrip antennas for SAR applications', *IEEE Trans. Antennas Propag.*, 1998, **46**, (9), pp. 1289–1296
2 Shafai, L.L., Chamma, W.A., Barakat, M., Strickland, P.C., Seguin, G.: 'Dual-band dual-polarized perforated microstrip antennas for SAR applications', *IEEE Trans. Antennas Propag.*, 2000, **48**, (1), pp. 58–66
3 Pozar, D.M., Targonski, S.D.: 'A shared-aperture dual-band dual-polarized microstrip array', *IEEE Trans. Antennas Propag.*, 2001, **49**, (2), pp. 150–157
4 Duffley, B.G., Morin, G.A., Mikavica, M., Antar, Y.M.M.: 'A wide-band printed double-sided dipole array', *IEEE Trans. Antennas Propag.*, 2004, **52**, (2), pp. 628–631
5 Eldek, A.A.: 'Design of double dipole antenna with enhanced usable bandwidth for wideband phased array applications', *Prog. Electromagn. Res.*, 2006, **59**, pp. 1–15
6 Qu, X., Zhong, S.S., Zhang, Y.M., Wang, W.: 'Design of an S/X dual-band dual-polarised microstrip antenna array for SAR applications', *IET Microw. Antennas Propag.*, 2007, **1**, (2), pp. 513–517
7 Lim, K.S., Tan, C.P., Lo, Y.C., Leong, W.S.: 'Design, construction and analysis of short-circuited and probe-fed microstrip based dipole arrays', *J. Electromagn. Waves Appl.*, 2008, **22**, (2–3), pp. 173–185
8 He, S., Xie, J.: 'Analysis and design of a novel dual-band array antenna with a low profile for 2400/5800-MHz WLAN systems', *IEEE Trans. Antennas Propag.*, 2010, **58**, (2), pp. 391–396
9 Floc'h, J.-M., Rmili, H.: 'Design of multiband printed dipole antennas using parasitic elements', *Microw. Opt. Technol. Lett.*, 2006, **48**, (8), pp. 1639–1645
10 Chen, W.-S., Yu, Y.-H.: 'Dual-band printed dipole antenna with parasitic element for WiMAX applications', *Electron. Lett.*, 2008, **44**, (23), pp. 1338–1339
11 Herraiz-Martinez, F.J., Garcia-Munoz, L.E., Segovia-Vargas, D., Gonzalez-Ovejero, D., Craeye, C.: 'Arrays of dual-band printed dipoles loaded with metamaterial particles'. Third European Conf. on Antennas and Propagation (EuCAP), Berlin, Germany, 2009, pp. 3818–3822
12 Gonzalez-Posadas, V., Jimenez-Martin, J.L., Herraiz-Martinez, F.J., Garcia-Munoz, L.E., Segovia-Vargas, D.: 'Design of dual-frequency SRR-loaded dipole with equivalent circuit approach', *Electron. Lett.*, 2009, **45**, (19), pp. 964–966
13 Baik, J.-W., Lee, T.-H., Pyo, S., Han, S.-M., Jeong, J., Kim, Y.-S.: 'Broadband circularly polarized crossed dipole with parasitic loop resonators and its arrays', *IEEE Trans. Antennas Propag.*, 2011, **59**, (1), pp. 80–88
14 Li, R., Wu, T., Pan, B., Lim, K., Laskar, J., Tentzeris, M.M.: 'Equivalent-circuit analysis of a broadband printed dipole with adjusted integrated balun and an array for base station applications', *IEEE Trans. Antennas Propag.*, 2009, **57**, (7), pp. 2180–2184

© The Institution of Engineering and Technology 2012

15 Xia, T., Yang, S., Nie, Z.: 'Design of a tapered balun for broadband arrays with closely spaced elements', *IEEE Antennas Wirel. Propag. Lett.*, 2009, **8**, pp. 1291–1294
16 Lin, S.-C., Jong, T.-L., Hsieh, C.-W., Ho, K.-J.: 'Wideband series-fed dipole antenna with balun integrated', *J. Electromagn. Waves Appl.*, 2010, **24**, (17–18), pp. 2463–2477
17 Sondas, A., Ucar, M.H.B., Erdemli, Y.E.: 'Dual-band loop-loaded printed dipole array'. Mediterranean Microwave Symp. (MMS), Guzelyurt, Turkish Republic of Northern Cyprus, 2010, pp. 62–64
18 Sondas, A., Ucar, M.H.B., Erdemli, Y.E.: 'Tunable loop-loaded printed dipole antenna design'. IEEE Int. Symp. Antennas Propagation, Toronto, Canada, 2010, pp. 1–4

© The Institution of Engineering and Technology 2012

doi: 10.1049/iet-map.2011.0244